Votano, J. R., Altman, J., Wilchek, M., Gorecki, M., & Rich, A. (1984) *Proc. Natl. Acad. Sci. U.S.A. 81*, 3190–3194.
Willard, J. M., Davis, J. J., & Wood, H. G. (1969) *Biochemistry 8*, 3137–3144.
Wishner, B. C., Hanson, J. C., Ringle, W. M., & Love, W. E. (1976) *Proceedings of the Symposium on Molecular and Cellular Aspects of Sickle Cell Disease* (Hercules, J. I., Cottam, G. L., Waterman, M. R., & Schechter, A. N., Eds.) pp 1–29, DHEW Publication No. 76-1007, NIH, Bethesda, MD.

Observation of Manganese(II)–Ligand Superhyperfine Couplings in Complexes with Proteins by Electron Spin-Echo Spectroscopy†

Russell LoBrutto,‡ Geoffrey W. Smithers,§ George H. Reed,*,§ William H. Orme-Johnson,∥ Swee L. Tan,∥ and John S. Leigh, Jr.*,‡

Department of Biochemistry and Biophysics, University of Pennsylvania School of Medicine, Philadelphia, Pennsylvania 19104, Institute for Enzyme Research, Graduate School, and Department of Biochemistry, College of Agricultural and Life Sciences, University of Wisconsin, Madison, Wisconsin 53705, and Department of Chemistry, Massachusetts Institute of Technology, Cambridge, Massachusetts 02139

Received November 20, 1985; Revised Manuscript Received March 26, 1986

ABSTRACT: Pulsed electron paramagnetic resonance spectroscopy has been used to detect Mn(II)–ligand superhyperfine couplings in complexes with creatine kinase and in the Mn(II) metalloprotein concanavalin A. Electron spin-echo envelopes from Mn(II), bound in these complexes, are modulated by superhyperfine interactions between Mn(II) and nearby, weakly coupled nuclear spins. The characteristic frequencies of the modulations were obtained by Fourier transformation of the three-pulse, spin-echo envelopes. In transition-state analogue complexes of creatine kinase (enzyme–Mn^{II}ADP–anion–creatine), superhyperfine interactions from the directly coordinated nitrogen of the thiocyanate ligand give envelope modulations. The source of the modulations was confirmed by measurements with the ^{14}N and ^{15}N forms of thiocyanate. On the other hand, the nitrogen of coordinated nitrate, which is two bonds removed from the paramagnetic center, does not produce detectable modulations. In spectra for Mn(II) concanavalin A, envelope modulations are detected due to the nitrogen of the coordinated histidine residue. Complexes prepared in ^2H_2O give strong signals due to weakly coupled ^2H. For Mn(II)-doped single crystals of sodium pyrophosphate, signals are observed in the frequency domain spectra that are due to coupling from ^{31}P. Phosphorus signals from the ADP ligand in complexes with creatine kinase show approximately the same coupling constant but have a much broader line width.

Divalent manganese is a popular paramagnetic probe for both NMR[1] and EPR investigations of metal ion binding sites and liganding interactions in enzymes and other proteins (Mildvan & Gupta, 1978; Reed & Markham, 1984). While Mn(II) is a natural constituent or specific activator of relatively few proteins (McEuen, 1982), it does function virtually isomorphically with respect to Mg(II) as an activator of many other enzymes (Reed & Markham, 1984). The long-lived spin states of this S-state ion are conducive to EPR measurements at room temperature and provide for enhanced rates of relaxation for nearby nuclear spins in macromolecular complexes. Superhyperfine interactions between the unpaired electron spin of Mn(II) and nuclear spins in the immediate vicinity of the ion provide a means for the unequivocal identification of ligands. For example, the high nuclear spin multiplicity ($I = {}^5/_2$) and the relatively strong, scalar superhyperfine coupling from ^{17}O of directly coordinated oxygen ligands result in significant changes in the line widths of Mn(II) EPR signals relative to those observed for ligands with ^{16}O (Reed & Leyh, 1980). Despite the generally favorable electron spin relaxation properties of the ion, however, EPR signals for complexes of Mn(II) with proteins typically have line widths that are too broad to permit detection of superhyperfine splittings from more weakly coupled nuclei. Thus, superhyperfine coupling between Mn(II) and nuclei such as ^{14}N or ^{15}N is normally concealed in the line widths of the EPR signals (Reed & Markham, 1984).

ENDOR (Scholes, 1979) and ESEEM (Norris et al., 1980; Mims & Peisach, 1981; Thomann et al., 1984) spectroscopies have the potential for detection of nuclear spin couplings that remain unresolved in a conventional EPR spectrum. In particular, the success of ESEEM spectroscopy, exemplified by recent studies of iron and copper metalloproteins (Mims & Peisach, 1976, 1979), prompted an investigation of the applicability of this methodology to studies of Mn(II) in complexes with proteins. The present paper reports the results of ESE measurements for Mn(II) in transition-state analogue complexes with creatine kinase and for the Mn(II) metalloprotein, concanavalin A.

† This work was supported by Grants AM 17517, AM 36842, and GM 35752 (G.H.R.), GM 25052 (J.S.L.), and GM 28358 (W.H.O.-J.) from the National Institutes of Health.

* Address correspondence to these authors.
‡ University of Pennsylvania.
§ University of Wisconsin.
∥ Massachusetts Institute of Technology.

[1] Abbreviations: NMR, nuclear magnetic resonance; EPR, electron paramagnetic resonance; ENDOR, electron nuclear double resonance; ESEEM, electron spin-echo envelope modulation; ESE, electron spin-echo; Hepes, 4-(2-hydroxyethyl)-1-piperazineethanesulfonic acid; S/N, signal-to-noise ratio; FFT, fast Fourier transform; H_1, magnetic field component of microwave radiation.

0006-2960/86/0425-5654$01.50/0

Experimental Procedures

Materials. Creatine kinase was isolated from rabbit skeletal muscle by method B of Kuby et al. (1954). Prior to use, the protein was chromatographed on a column (2.5 × 95 cm) of Sephacryl S-200 (Pharmacia) equilibrated with 50 mM Hepes–KOH, pH 8.0, and concentrated with a collodion bag apparatus. Enzyme prepared in this manner had a specific activity of >40 IU/mg protein when measured in the coupled assay (Tanzer & Gilvarg, 1959) at 25 °C. Jack bean concanavalin A (type IV: lyophilized powder, essentially salt free) was obtained from Sigma Chemical Co. and was used without further purification. Single crystals of $Na_4P_2O_7 \cdot 10H_2O$ were grown from saturated aqueous solutions of sodium pyrophosphate containing 0.1% (w/w) $MnCl_2$. ADP (Sigma) was purified by chromatography on DEAE-Sephadex (A-25) (Pharmacia) and Chelex-100 (Bio-Rad) as described previously (Reed & Leyh, 1980; Smithers & O'Sullivan, 1982). Deuterium oxide (99.7 atom % ^2H) was obtained from Merck Sharp & Dohme, and $Na^{15}NO_3$ (99.1 atom % ^{15}N) and $KC^{15}N$ (95.0 atom % ^{15}N) were purchased from Prochem. The potassium salt of thiocyanate (enriched with ^{15}N) was prepared from elemental sulfur and $KC^{15}N$ as described by Sternlicht et al. (1971). X-band EPR spectra for the complexes in frozen solution had the same appearance as those obtained in the solution phase.

ESEEM Spectroscopy. The basic design of the ESE spectrometer was patterned after that described by Norris et al. (1980). The spectrometer employed a magnet and field controller from a modified Varian E-4 EPR spectrometer. The frequency source was a 50-mW Gunn oscillator that operated between 8.8 and 9.4 GHz. The output from the oscillator was amplified to 38 W with a traveling wave tube (ITT). The noise output from the traveling wave tube, following the pulses, was blocked by a custom-made, narrow-band (nominally 9.0–9.2 GHz) PIN switch (Triangle Microwave) that could handle a throughput of up to 50 W in short pulses.

A custom-built, microwave resonator with a large filling factor compensated for the modest microwave power levels from the traveling wave tube amplifier. The microwave resonator[2] (see Figure 1) consists of a strip of copper foil, 3.7 mm × 10.8 mm, wrapped around a 4-mm (o.d.) quartz sample tube. The tube was placed into the flow Dewar, which was encased in a 12.4-mm (i.d.) cylindrical brass shield with an open slot over which an iris/waveguide was attached. The Q of the resonator (4000 critically coupled) was reduced to the required range (<400) for ESE measurements by overcoupling the resonator to the waveguide through use of an iris with a square coupling hole. Frequency shifts produced by small conducting objects indicated that the H_1 field was parallel to the long axis of the sample tube. The 20–25-ns duration for a 90° pulse indicated that the H_1 field at the sample reached a magnitude of approximately 4 G.

The ESE signal was amplified by a limiter-protected, GaAs FET amplifier (Narda) with a nominal 3.5-dB noise figure and combined in a double-balanced mixer with power from the Gunn oscillator that was routed through the reference arm. The video output was taken directly into a boxcar integrator (Stanford Research Systems). The dc output from the integrator was amplified (Tektronix differential amplifier) and digitized with a Data Translations analog–digital interface board for an IBM PC computer.

[2] A more detailed description of the spectrometer and a detailed description of the resonator, including electrical properties (measured and calculated), are available from R.L.B. or J.S.L. on request.

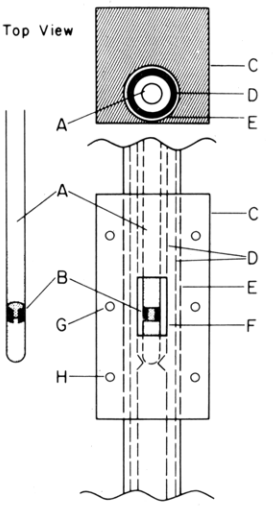

FIGURE 1: Schematic representation of the current sheet microwave resonator with flow Dewar and special shield. The features depicted are (A) sample tube, 4-mm (o.d.); (B) 0.001-in. copper foil resonator, 10.6 mm × 3.5 mm; (C) brass block, 25.4 mm square × 50.8 mm high; (D) double-walled quartz flow Dewar; (E) inner bore of brass shield, 12.6-mm diameter (inner bore is extended 50 mm above and 25 mm below the block with brass tubing, soldered into place); (F) slot in shield wall, 6.5 mm × 12 mm; (G) threaded holes for fastening iris over slot; (H) holes for fastening waveguide over iris.

Scan times of approximately 30 s were used with a pulse repetition rate of 833 Hz so that each point in a single 1024-point scan represents a sum over 24 repetitions. Between 64 and 96 scans were used to accumulate each spectrum.

A temperature near 7.5 °K was selected for most of the ESE measurements. This temperature represents an operational optimum with respect to echo amplitudes and consumption of liquid helium. The echo amplitudes[3] do, however, diminish appreciably at higher temperatures.

A three-pulse "stimulated echo" sequence (90°–τ–90°–T–90°–τ–echo) was used (Mims & Peisach, 1978; Norris et al., 1980), where τ was fixed and T was continuously varied. The interval between the first two pulses, τ, was also varied with each sample to ensure that there were no frequencies that were arbitrarily nulled by the pulse spacing. Envelope modulation spectra were analyzed, in part, by computation of the FFT of the modulations.[4] Prior to FFT computation, the echo envelopes were fitted to single exponentials, which were then subtracted from the envelopes. In each case, the absolute value form of the cosine transform was used to generate the frequency spectrum.

[3] The electron spin echoes provide the carrier upon which nuclear modulations are observed, and the S/N ratio in the echoes is therefore one important factor in obtaining good S/N in ESEEM spectra. S/N ratios in the frequency domain of the envelope modulations are, however, also governed by the depths of the modulations, and it is possible to have a high S/N ratio in the echo signal with weak modulations. Partial excitation of the hyperfine manifold (Barkhuijsen et al., 1985), due to an insufficient H_1 field in the microwave pulse, is one factor that can limit the depth of modulations. The 2-fold higher H_1 field from the ESE spectrometer at the Massachusetts Institute of Technology did not enhance the depths of modulations due to nitrogen nuclear spins over those observed from the same samples with the lower power spectrometer. It is therefore unlikely that partial excitation is limiting the depths of modulations due to coupled nitrogens.

[4] The initial portion of the echo envelope (i.e., that coincident with the dead-time of the spectrometer), was arbitrarily set to zero. The remaining data were fitted to an exponential that was removed prior to Fourier transformation. Simulations show that this procedure does not introduce spurious frequencies of significant amplitude or appreciable distortions in line shape into the frequency spectrum, except for an artifact that occurs near zero frequency.

For measurements of ^{31}P couplings from ADP in complexes with creatine kinase, the high-power (1-kW) ESE spectrometer at the Massachusetts Institute of Technology was used. This instrument employs a rectangular cavity (with an enlarged iris to facilitate overcoupling and thereby a reduction in Q) as a probe. The 90° pulse lengths of 10–15 ns obtained with this spectrometer translate into H_1 fields between 6 and 9 G. In these experiments, the three-pulse echo envelopes were fitted to cubic spline functions (Nicolet Instruments, Inc.) prior to Fourier transformation.

The strongest EPR signals in the powder pattern spectra for Mn(II) in macromolecular complexes come from the central fine structure transition ($M_s = {}^1/_2 \leftrightarrow M_s = -{}^1/_2$). The six ^{55}Mn hyperfine components of this transition contain additional structure due to second-order and higher order effects from the zero-field splitting interaction. These anisotropic splittings map the orientation dependence resulting from the zero-field splitting interaction (Reed & Markham, 1984). The region of the spectrum for ESEEM measurements was selected by scanning the magnetic field to locate positions where the spin echoes showed the strongest modulations. Modulations of varying strengths were normally observed throughout the region of the magnetic field encompassing the central fine-structure transition. The width of the microwave pulse was sufficient to "burn a hole" approximately 4 G wide in the absorption envelope. Depending on the position of the magnetic field, the microwave pulse may sample a fairly narrow distribution of molecular orientations. The corresponding frequency-domain ESEEM spectra are, therefore, not "pure" powder patterns for the nuclear spin transitions.

Frequency spectra were obtained by Fourier transformation of the spin-echo envelope modulations. Signals arising from $I = {}^1/_2$ nuclei (e.g., ^{15}N and ^{31}P) were analyzed with the first-order expressions from ENDOR spectroscopy (Scholes, 1979). For a nuclear spin of ${}^1/_2$, the two ENDOR frequencies are given by

for ${}^1/_2|A| > g_n\beta_n H$

$$h\nu_{obsd} = {}^1/_2|A| \pm g_n\beta_n H \quad (1a)$$

and for ${}^1/_2|A| < g_n\beta_n H$

$$h\nu_{obsd} = g_n\beta_n H \pm {}^1/_2|A| \quad (1b)$$

Here, the hyperfine coupling parameter, A, is the sum of the isotropic and anisotropic components, ν_{obsd} is the observed frequency, and $g_n\beta_n H$ is the nuclear Zeeman interaction term.

Analysis of ESEEM spectra for ^{14}N ($I = 1$) is complicated by the nuclear quadrupole interaction (Mims & Peisach, 1978). In ENDOR spectroscopy the ^{14}N nucleus can give rise to four frequencies corresponding to $\Delta m_I = \pm 1$ transitions within the two nuclear spin manifolds associated with the $+{}^1/_2$ and $-{}^1/_2$ electron spin states (Scholes, 1979). The frequencies of these transitions for the case ${}^1/_2|A| > g_n\beta_n H$, P, where P is the nuclear quadrupolar interaction term, are given by the first-order expression

$$h\nu_{obsd} = {}^1/_2|A| \pm |P| \pm g_n\beta_n H \quad (2)$$

However, two additional modulation frequencies corresponding to $\Delta m_I = \pm 2$ transitions have been observed in ESEEM studies of Cu(II) (Mims & Peisach, 1978) and Fe(III) (Peisach et al., 1979) complexes. Thus, six frequencies may contribute to the modulation of the echo envelopes. In a powder sample, signals corresponding to the $\Delta m_I = 1$ transitions may have broader widths because of the orientation dependence of the nuclear spin levels. Quantitative assignments of the ESEEM signals for ^{14}N are, therefore, complicated, especially in the absence of independent information regarding the magnitude of the quadrupolar coupling. In the present applications, couplings from ^{14}N have been qualitatively identified either by direct comparison with spectra for matched samples with ^{15}N (complexes with creatine kinase) or by the range of frequencies observed combined with independent knowledge of nitrogen coordination (concanavalin A).

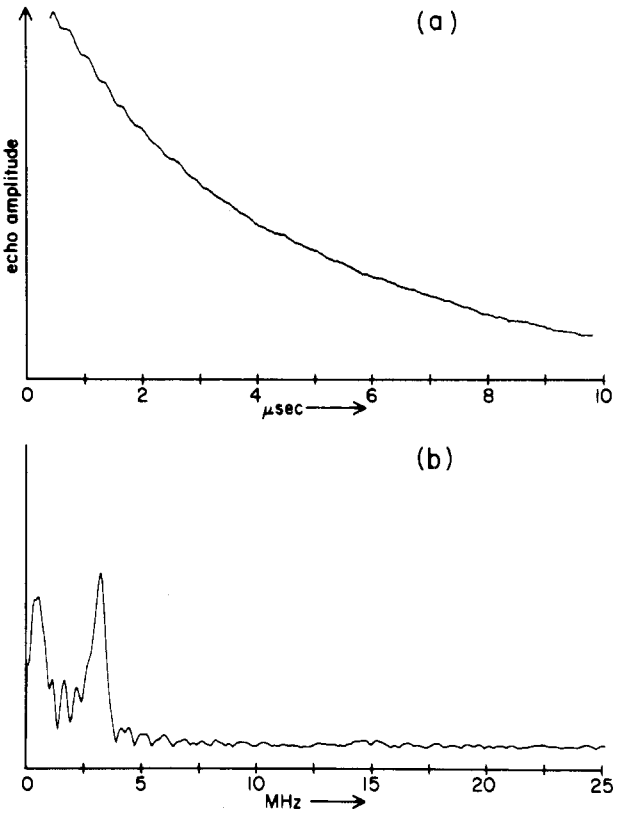

FIGURE 2: Three-pulse electron spin-echo envelope (a) and Fourier transform of the envelope modulation (b) for the creatine kinase–Mn^{II}ADP–$^{15}NCS^-$–creatine complex. The time-domain spectrum was recorded at 8 K with a microwave frequency of 9.058 GHz, a magnetic field of 3480 G, and τ = 200 ns. The sample contained 3.0 mM enzyme active sites, 1.5 mM $Mn(acetate)_2$, 4.0 mM ADP, 50.0 mM $K^{15}NCS$, saturating creatine, and 50 mM Hepes–KOH, pH 8.0.

RESULTS

Complexes with Creatine Kinase. The dead-end complex formed by the combination of creatine kinase, Mn^{II}ADP, and creatine is stabilized by a class of planar anions that take up the position normally occupied by the transferring phospho group (i.e., the γ-phosphate of ATP or the phosphoguanidinium group of phosphocreatine). These anion-stabilized complexes may be viewed as analogues of the transition state of the reaction (Milner-White & Watts, 1971; Kenyon & Reed, 1983). Infrared (Reed et al., 1978) and EPR (Reed & Leyh, 1980) measurements have shown that the anions contribute a ligand to the metal ion in such complexes. These inhibitory anions provide convenient vehicles for bringing nuclear spin probes into the immediate vicinity of the bound Mn(II).

The three-pulse echo envelope for a sample of the transition-state analogue complex, creatine kinase–Mn^{II}ADP–$^{15}NCS^-$–creatine, and the Fourier transform of the envelope are shown in Figure 2. Spectra obtained for a matched sample of the corresponding enzymic complex containing $^{14}NCS^-$ are given in Figure 3. The clear differences in the time-domain spectra for the two enzymic complexes containing either

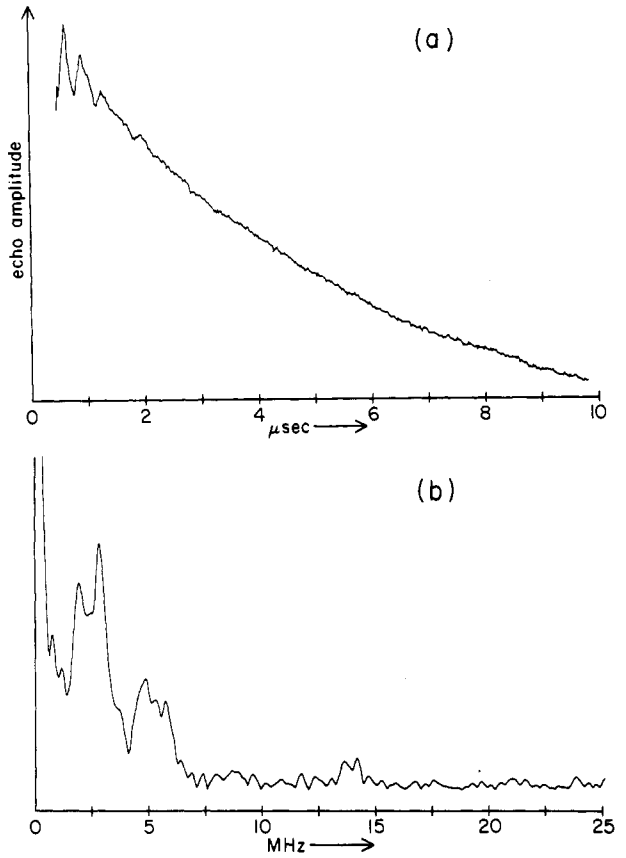

FIGURE 3: Three-pulse electron spin-echo envelope (a) and Fourier transform of the envelope modulation (b) for the creatine kinase–$Mn^{II}ADP$–$^{14}NCS^-$–creatine complex. The time-domain spectrum was recorded at 8 K with a microwave frequency of 8.894 GHz, a magnetic field of 3410 G, and τ = 140 ns. The sample contained 3.0 mM enzyme active sites, 1.5 mM $Mn(acetate)_2$, 4.0 mM ADP, 50.0 mM $K^{14}NCS$, saturating creatine, and 50 mM Hepes–KOH, pH 8.0.

$^{15}NCS^-$ or $^{14}NCS^-$ (compare Figures 2a and 3a) show that the source of the modulations is the nitrogen of the NCS^- ligand. The signal at 3.4 MHz in the spectrum for the complex with $^{15}NCS^-$ is one component of the ^{15}N doublet (see eq 1a), the other component being spaced either at $+2g_n\beta_nH$ or at $-2g_n\beta_nH$ (3 MHz) from this signal. The low-frequency extreme of the spectrum contains an artifact[4] that would partially overlap with the potential 0.4-MHz resonance of ^{15}N. The spectrum is, however, flat in the region of 6.4 MHz, so the shoulder at 0.4 MHz appears to be the missing component of the ^{15}N doublet. The apparent hyperfine coupling parameter (3.8 MHz) is given by the sum of the two transition frequencies (Table I).

Modulations from the sample with $^{14}NCS^-$ are weaker than those observed for the sample containing $^{15}NCS^-$, and this reduces the S/N ratio of the frequency-domain spectrum (Figure 3b). The hyperfine coupling parameter (2.7 MHz) may be calculated from the experimental result for the complex with $^{15}NCS^-$ (Table I). The frequencies of the major features in Figure 3b, however, cannot be predicted with eq 2. It is therefore likely that at least one, and possibly two, of these frequencies correspond to $\Delta m_I = 2$ nuclear spin transitions (Mims & Peisach, 1978). Although nuclear quadrupole resonance data for some N-bonded thiocyanate complexes are available (Cheng et al., 1977), the low S/N ratio in Figure 3b precludes a more quantitative assignment of the quadrupole coupling parameters.

In contrast to the results obtained for the complexes with thiocyanate, the nitrogen (either ^{14}N or ^{15}N) of coordinated nitrate in the enzyme–$Mn^{II}ADP$–NO_3^-–creatine complex does not give observable modulations in the echo envelopes. In fact, both the time-domain and frequency-domain spectra for this complex are almost featureless (Figure 4a,b). The absence of modulations from nitrogen nuclei in the ESEEM spectra for the nitrate complex, however, provides a reasonably clear window for investigation of deuterium couplings in ^2H_2O. The spin-echo envelope for the complex, creatine kinase–$Mn^{II}ADP$–$^{14}NO_3^-$–creatine in ^2H_2O (Figure 4c) exhibits strong modulations, and the frequency-domain spectrum (Figure 4d) reveals an intense signal centered at the free ^2H frequency (2.30 MHz). This signal most likely includes contributions from the "matrix" of exchangeable deuterons,

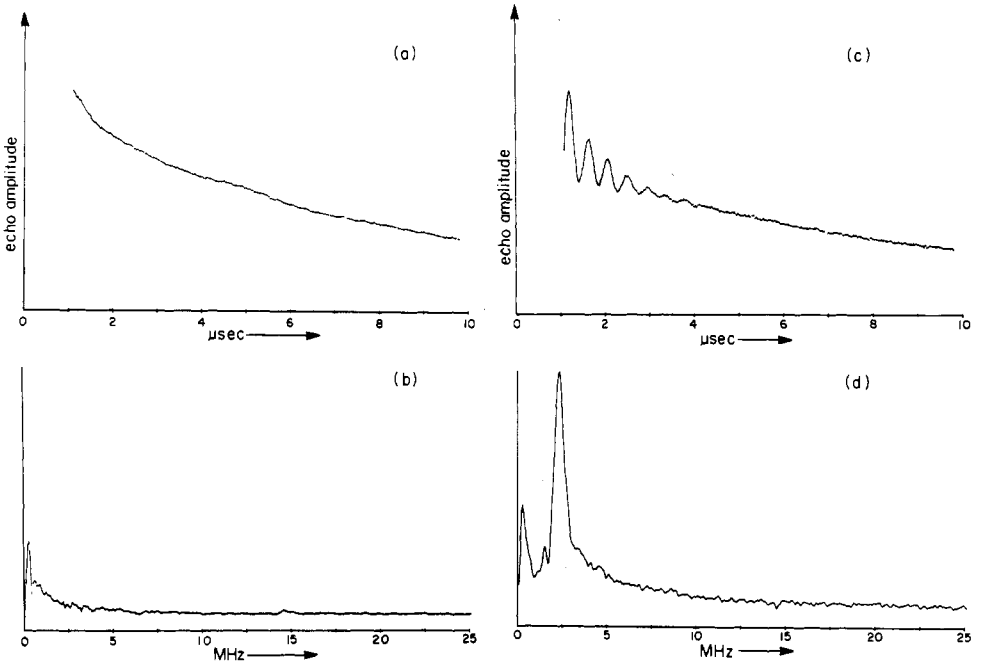

FIGURE 4: Three-pulse electron spin-echo envelopes (a, c) and Fourier transforms of the envelope modulations (b, d) for the creatine kinase–$Mn^{II}ADP$–$^{14}NO_3^-$–creatine complex prepared in H_2O (a, b) and ^2H_2O (c, d). The time-domain spectra were recorded at 7.5 K with microwave frequencies of 9.07 (a) and 9.10 GHz (c), a magnetic field of 3450 G, and τ = 230 ns. The samples contained 1.37 mM enzyme active sites, 0.70 mM $Mn(acetate)_2$, 3.0 mM ADP, 60.0 mM $K^{14}NO_3$, saturating creatine, and 50 mM Hepes–KOH, pH 8.0.

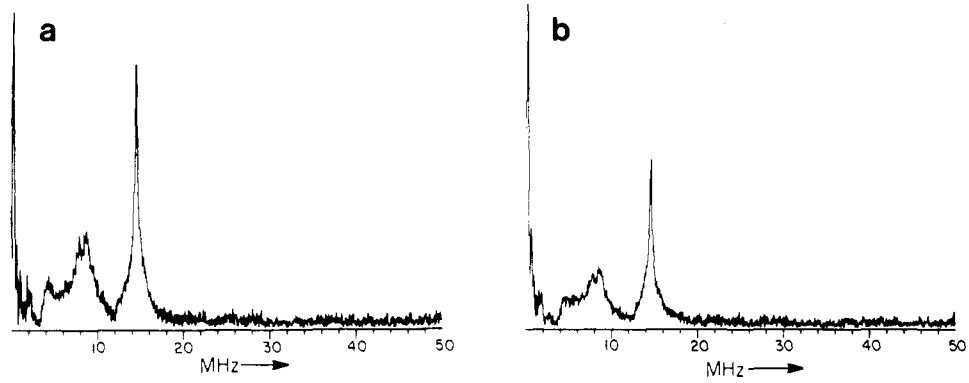

FIGURE 5: Fourier transforms of the envelope modulations for the creatine kinase–Mn^{II}ADP–NO_3^-–creatine complex containing $^{14}NO_3^-$ (a) or $^{15}NO_3^-$ (b). The spectra were recorded with the high-power ESE spectrometer (see Experimental Procedures) at 15 K, using a microwave frequency of 9.14 GHz, a magnetic field of 3560 G, and τ = 170 ns. The samples contained 3.0 mM enzyme active sites, 1.3 mM $Mn(acetate)_2$, 4.0 mM ADP, 10.0 mM $K^{14}NO_3$ or $K^{15}NO_3$, saturating creatine, and 50 mM Hepes–KOH, pH 8.0.

Table I: Frequencies of Major Signals and Coupling Parameters for Nuclei in Mn(II) Complexes with Creatine Kinase and Concanavalin A

complex[a]	ligand	nucleus	ν_{obsd} (MHz)	A (MHz)[b]
creatine kinase–Mn^{II}ADP–NCS^-–creatine	$^{15}NCS^-$	^{15}N	0.4 ± 0.2 3.4 ± 0.1	3.8 ± 0.1
	$^{14}NCS^-$	^{14}N	2.0 ± 0.3 2.9 ± 0.1 4.9 ± 0.3	(2.7 ± 0.2)[c]
creatine kinase–Mn^{II}ADP–NO_3^-–creatine	ADP	^{31}P	4.0–8.0	(4.0 ± 0.5)[d]
Mn(II) concanavalin A	histidine	^{14}N	2.8 ± 0.2 5.0 ± 0.2	

[a] The concentrations of components in the respective complexes can be found in the figure legends. [b] Hyperfine coupling parameter. In most cases this parameter is approximately equal to the scalar superhyperfine coupling constant (see text). [c] Calculated from the ^{15}N coupling ($A^{14}_N = A^{15}_N\gamma^{14}_N/\gamma^{15}_N$). [d] Maximum coupling.

but the width of the resonance is sufficient to encompass contributions from the more strongly coupled ^2H of the water ligands.

Frequency-domain spectra for the samples with nitrate exhibit a very broad, weak feature in the region close to 6 MHz. This broad feature was much stronger in spectra obtained for these samples with the high-power ESE spectrometer (Figure 5). The frequency-domain spectrum for the nitrate complex (Figure 5a) reveals broad peaks at 4 and 8 MHz. The corresponding spectrum from the $^{15}NO_3^-$ samples (Figure 5b) gives the same feature, so these resonances are not signals from nitrogen. These signals are centered about the ^{31}P Larmor frequency (6.03 MHz at 3500 G) and are tentatively assigned to ^{31}P from the ADP ligand.

The characteristics of ^{31}P–Mn(II) coupling were also investigated with an inorganic crystal. Single crystals of $Na_4P_2O_7{\cdot}10H_2O$ doped with 0.1% $MnCl_2$ yield sharp EPR signals for the Mn(II) impurity.[5] The three-pulse echo envelope for a single crystal shows deep modulations (Figure 6a). Within the central fine structure transition and with the magnetic field along the crystallographic a axis (MacArthur & Beevers, 1957), the two dominant frequencies in the spectrum (Figure 6b) exhibit a field dependence that is expected for the magnetogyric ratio of ^{31}P. The ^{31}P doublet splitting remained virtually constant within the ac plane. Although the coupling constant of 4 MHz obtained from the single-crystal specimen correlates with that observed for the enzymic complex, the much broader line widths for the ^{31}P signals in the spectrum for the latter complex are not yet understood.

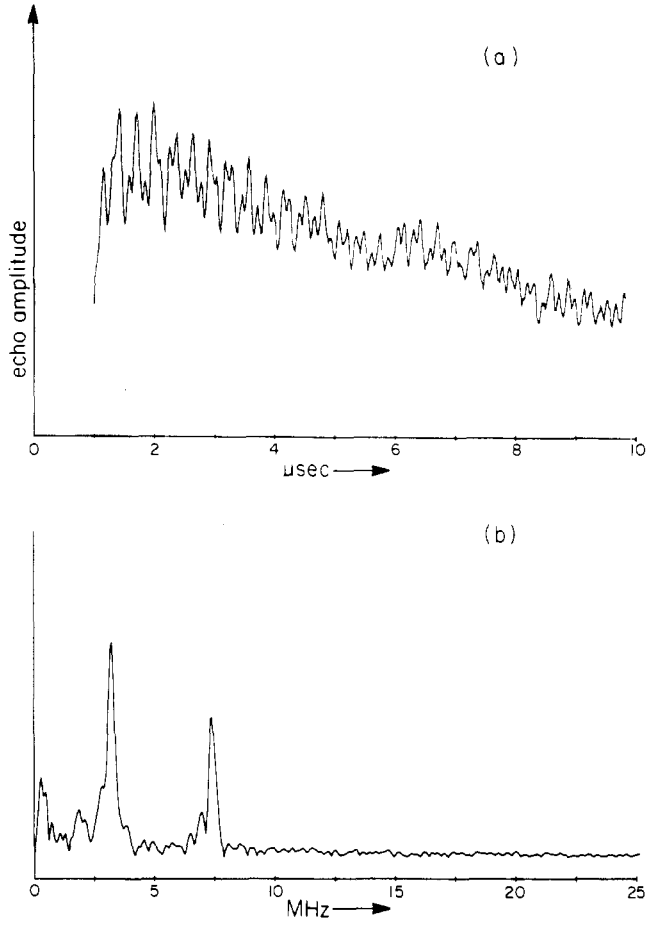

FIGURE 6: Three-pulse electron spin-echo envelope (a) and Fourier transform of the envelope modulation (b) for $MnCl_2$ doped (0.1% (w/w)) into a single crystal of $Na_4P_2O_7{\cdot}10H_2O$. The time-domain spectrum was recorded at 8 K, with the magnetic field (3250 G) lying along the crystallographic a axis (the shorter edge of the prominent crystal face), using a microwave frequency of 9.16 GHz and τ = 320 ns.

Attempts to observe ESEEM from ^{17}O (40 atom % enrichment) in the phosphate groups of ADP were without success. ESEEM spectra for samples of the complexes creatine kinase–$Mn^{II}[\beta\text{-}^{17}O_3]$ADP–$HCOO^-$–creatine and creatine ki-

[5] Attempts to prepare a powder sample of the doped sodium pyrophosphate for comparison with the powder pattern spectrum for the enzymic complex were unsuccessful because grinding of the crystal led to magnetic concentration of the Mn(II) and exchange-narrowed EPR signals.

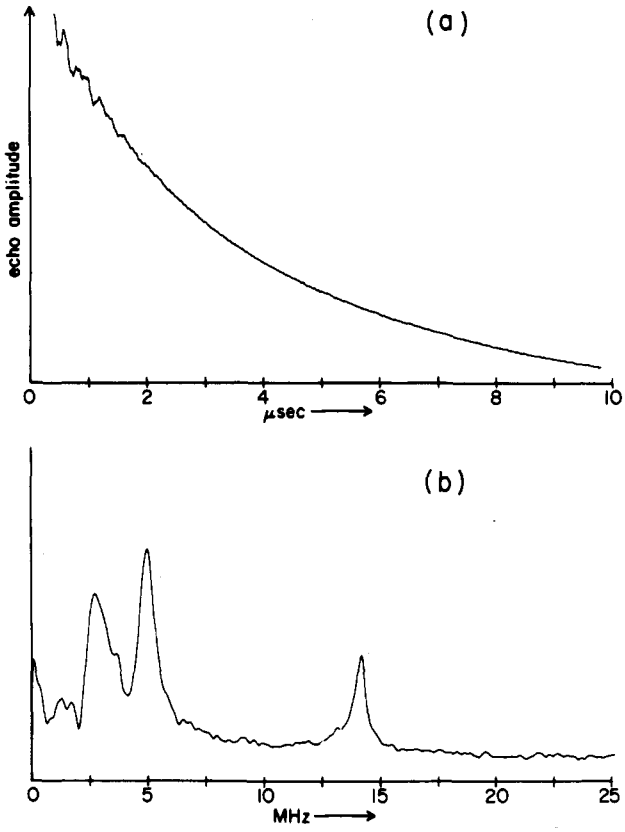

FIGURE 7: Three-pulse electron spin-echo envelope (a) and Fourier transform of the envelope modulation (b) for the Mn(II) concanavalin A complex. The time-domain spectrum was recorded at 7.5 K with a microwave frequency of 8.867 GHz, a magnetic field of 3383 G, and τ = 240 ns. The sample contained 30 mg of protein dissolved in 0.3 mL of 50 mM Hepes–KOH, pH 8.0.

nase–Mn^{II}[β-$^{17}O_3$]ADP–NO_3^-–creatine were featureless except for a weak proton signal. These two samples have ^{17}O in both coordinated and noncoordinated positions of the β-phosphate group. ESEEM spectra for the enzymic complex with [$\beta\gamma$-^{17}O]ATP (i.e., ^{17}O enrichment in the β,γ bridging oxygen where ^{17}O is exclusively noncoordinated) also failed to show evidence of modulation due to ^{17}O, even with the high-power ESE spectrometer.

Mn(II) Concanavalin A. The three-pulse echo envelope obtained from the highest-field peak of the ^{55}Mn hyperfine manifold (3492 G at 9.145 GHz) for a sample of concanavalin A is presented in Figure 7a, and the Fourier transform of the envelope is depicted in Figure 7b. The crystal structure of concanavalin A (0.24-nm resolution) shows that Mn(II) is coordinated to a nitrogen from His 24 (Reeke et al., 1974). The two most prominent features in the frequency-domain spectrum (2.8 and 5.0 MHz) are consistent with ^{14}N frequencies from the coordinated histidine residue.

Discussion

Instrumental and theoretical conditions for observation of nuclear modulation effects in electron spin-echo envelopes (see Mims & Peisach, 1981) are best met by weakly coupled spins. Strong scalar superhyperfine coupling results in a wider superhyperfine manifold that requires stronger microwave pulses, and a dominant scalar term weakens the semiforbidden transitions to the extent that they do not contribute appreciable interference effects. The absence of a dominant scalar term may not be as great a limitation for complexes of Mn(II) as it is for complexes of Cu(II) because ligand superhyperfine coupling constants are typically much smaller for complexes of Mn(II) (Goodman & Raynor, 1970).

Although thiocyanate is an ambidentate ligand, infrared data for the complex creatine kinase–Mn^{II}ADP–NCS^-–creatine are consistent with an N-bonded isomer of the thiocyanate ligand (Reed et al., 1978), as expected for a first-row transition-metal ion in a low oxidation state (Burmeister, 1975). Mn(II)–sulfur coordination reduces the magnitude of the ^{55}Mn hyperfine coupling (Van Wieringen, 1955; Lifshitz & Francis, 1982; Reed & Markham, 1984). The ^{55}Mn hyperfine coupling constant in EPR spectra for the complex with thiocyanate is, however, normal for oxygen and nitrogen ligands. Hence, the observed coupling must be due to a directly bonded nitrogen. The magnitude of the superhyperfine coupling between Mn(II) and the ^{15}N of thiocyanate (3.8 MHz) is significantly greater than the pure dipolar coupling calculated for a bond distance of 0.21–0.25 nm. This predominantly scalar coupling is compatible with an expected sp hybrid orbital of the nitrogen contributing to a Mn–N σ bond (Burmeister, 1975).

The deuterium signal that appears in the ESEEM spectra for samples in ^2H_2O and the proton signals that appear in virtually all of the spectra (near 15 MHz) provide examples of modulation from "remote" nuclei. There are three water ligands bound to Mn(II) in the transition-state analogue complexes with creatine kinase (Reed & Leyh, 1980). The broad ^2H signal obtained from the sample in ^2H_2O likely contains contributions from ^2H of the coordinated solvent. On the other hand, observation of ESEEM from the ^{31}P nuclei of the ADP ligand requires higher microwave powers. The line widths of these ^{31}P signals are not understood although the magnitude of the ^{31}P coupling constant is compatible with the results from ESEEM measurements on single crystals of Mn(II)-doped sodium pyrophosphate and from ^{31}P NMR data (Mays, 1963) for $LiMnPO_4$.

The absence of detectable modulations from directly coordinated ^{17}O is understandable given the fact that the scalar component of the ^{17}O superhyperfine tensor for coordinated oxygens is between 6 and 12 MHz (Zetter et al., 1978; Reed & Leyh, 1980). The microwave pulse from the low-power instrument is, therefore, too narrow to span the resulting sextet of the ^{17}O superhyperfine manifold in the EPR absorption envelope. Moreover, the semiforbidden transitions of the strongly coupled ^{17}O may be too weakly allowed to produce a significant modulation effect (Mims & Peisach, 1981). Even for unliganded ^{17}O nuclei, the pattern of ^{17}O nuclear spin transitions may be spread out over such a wide range of frequencies that the interaction is difficult to detect.

Superhyperfine couplings between Mn(II) and the nitrogens of the His 24 ligand are too weak to be resolved in EPR spectra for single crystals of the concanavalin A complex where the EPR signals have line widths of the order of 8–10 G (Meirovitch et al., 1974). The line widths of the EPR signals place an upper limit of approximately 6–8 MHz on the magnitude of the superhyperfine coupling to the coordinated nitrogen. This contrasts sharply with the >30-MHz scalar superhyperfine coupling between Cu(II) and ^{14}N of coordinated ligands (Maki & McGarvey, 1958; Kivelson & Neiman, 1961). The highest frequency observed in ESEEM spectra for concanavalin A is 5.1 MHz, and the range of frequencies is similar to that observed for the complex of creatine kinase with $^{14}NCS^-$, where a 2.7-MHz superhyperfine coupling is present. Thus, the signals in the ESEEM spectra for concanavalin A probably come from the ^{14}N of the coordinated nitrogen of His 24. Spin delocalization onto the His ligand is likely too small to allow appreciable hyperfine interaction with the unliganded nitrogen of the imidazole ring. By contrast, a

pseudodipolar coupling between spin density, transferred to the imidazole ring, and the remote nitrogen is responsible for the modulation effects in Cu(II)–imidazole complexes (Mims & Peisach, 1978).

Results presented here indicate that the ESEEM phenomenon for complexes of Mn(II) will be of a shorter range than for complexes of Cu(II) because of the less extensive spin delocalization. ESEEM spectroscopy will be particularly useful in detection of superhyperfine interactions from directly coordinated nitrogen. Paired measurements with complexes containing ligands with the two nuclides of nitrogen can provide an unambiguous means for identification of nitrogen ligands.

ACKNOWLEDGMENTS

We thank Dr. G. L. Kenyon for the sample of [$\beta\gamma$-^{17}O]ATP and J. L. Kofron for the Mn(II)-doped crystals of sodium pyrophosphate.

Registry No. ADP, 58-64-0; Mn, 7439-96-5; NCS^-, 302-04-5; D_2, 7782-39-0; ^{31}P, 7723-14-0; $Na_4P_2O_7 \cdot 10H_2O$, 13472-36-1; L-histidine, 71-00-1.

REFERENCES

Barkhuijsen, H., De Beer, R., Pronk, B. J., & Van Ormondt, D. (1985) *J. Magn. Reson. 61*, 284–293.

Burmeister, J. L. (1975) in *The Chemistry and Biochemistry of Thiocyanic Acid and Its Derivatives* (Newman, A. A., Ed.) pp 68–130, Academic, London.

Cheng, C. P., Brown, T. L., Fultz, W. C., & Burmeister, J. L. (1977) *J. Chem. Soc., Chem. Commun.*, 599–600.

Goodman, B. A., & Raynor, J. B. (1970) *Adv. Inorg. Chem. Radiochem. 13*, 135–362.

Kenyon, G. L., & Reed, G. H. (1983) *Adv. Enzymol. Relat. Areas Mol. Biol. 54*, 367–426.

Kivelson, D., & Neiman, R. (1961) *J. Chem. Phys. 35*, 149–155.

Lifshitz, E., & Francis, A. H. (1982) *J. Phys. Chem. 86*, 4714–4718.

Kuby, S. A., Noda, L., & Lardy, H. A. (1954) *J. Biol. Chem. 209*, 203–210.

MacArthur, D. M., & Beevers, C. A. (1957) *Acta Crystallogr. 10*, 428–432.

Maki, A. H., & McGarvey, B. R. (1958) *J. Chem. Phys. 29*, 35–38.

Mays, J. M. (1963) *Phys. Rev. 131*, 38–53.

McEuen, A. R. (1982) *Inorg. Biochem. 3*, 314–343.

Meirovitch, E., Luz, Z., & Kalb, A. J. (1974) *J. Am. Chem. Soc. 96*, 7538–7542.

Mildvan, A. S., & Gupta, R. K. (1978) *Methods Enzymol. 49*, 322–359.

Milner-White, E. J., & Watts, D. C. (1971) *Biochem. J. 122*, 727–740.

Mims, W. B., & Peisach, J. (1976) *Biochemistry 15*, 3863–3869.

Mims, W. B., & Peisach, J. (1978) *J. Chem. Phys. 69*, 4921–4930.

Mims, W. B., & Peisach, J. (1979) *J. Biol. Chem. 254*, 4321–4323.

Mims, W. B., & Peisach, J. (1981) *Biol. Magn. Reson. 3*, 213–263.

Norris, J. R., Thurnauer, M. C., & Bowman, M. K. (1980) *Adv. Biol. Med. Phys. 17*, 365–416.

Peisach, J., Mims, W. B., & Davis, J. L. (1979) *J. Biol. Chem. 254*, 12 379–12 389.

Reed, G. H., & Leyh, T. S. (1980) *Biochemistry 19*, 5472–5480.

Reed, G. H., & Markham, G. D. (1984) *Biol. Magn. Reson. 6*, 73–142.

Reed, G. H., Barlow, C. H., & Burns, R. A., Jr. (1978) *J. Biol. Chem. 253*, 4153–4158.

Reeke, G. N., Jr., Becker, J. W., Cunningham, B. A., Gunther, G. R., Wang, J. L., & Edelman, G. M. (1974) *Ann. N.Y. Acad. Sci. 234*, 369–382.

Scholes, C. P. (1979) in *Multiple Electron Resonance Spectroscopy* (Dorio, M. M., & Freed, J. H., Eds.) pp 297–330, Plenum, New York.

Smithers, G. W., & O'Sullivan, W. J. (1982) *J. Biol. Chem. 257*, 6164–6170.

Sternlicht, H., Kenyon, G. L., Packer, E. L., & Sinclair, J. (1971) *J. Am. Chem. Soc. 93*, 199–208.

Tanzer, M. L., & Gilvarg, C. (1959) *J. Biol. Chem. 234*, 3201–3204.

Thomann, H., Dalton, L. R., & Dalton, L. A. (1984) *Biol. Magn. Reson. 6*, 143–186.

Van Wieringen, J. S. (1955) *Discuss. Faraday Soc. 19*, 118–126.

Zetter, M. S., Lo, G. Y.-S., Dodgen, H. W., & Hunt, J. P. (1978) *J. Am. Chem. Soc. 100*, 4430–4436.